Colloid & Polymer Science Colloid Polym Sci 267:311–322(1989)

On the decisive role of finite chain extensibility and global interactions in networks

M. Zrinyi[1]), H.-G. Kilian, and F. Horkay[1])

Abteilung Experimentelle Physik, Universität Ulm, Ulm, FRG
[1]) Department of Colloid Science, L. Eötvös University, Budapest, Hungary

Abstract: The stress-strain dependence of dry networks at unidirectional extension and compression is studied. The phenomenological van der Waals equation of state is compared with different molecular models in order to provide an interpretation of the van der Waals corrections. It is shown that the stress-strain behavior predicted by the phantom, Langevin, and constrained junction fluctuation models are altogether covered by the van der Waals approach. The relationship between the suppression of junction fluctuation parameter introduced by Dossin and Graessley and the van der Waals corrections has been worked out. The effect of junction functionality on the small strain modulus as well as on the second Mooney-Rivlin coefficient is also presented.

Key words: Polymer networks, van der Waals approach, phantom network, Langevin network, constrained junction fluctuation model, Mooney-Rivlin coefficients, simple extension, unidirectional compression, poly(vinyl acetate) network.

Introduction

According to the Gaussian theories of rubber elasticity, the network is considered as a permanently linked assembly of independent entropic springs represented by volumeless phantom chains [1, 2]. Regarding the fluctuation of junctions, two physically different approaches have been introduced:

1) In the affine network model it is assumed that the junctions do not fluctuate at all. As a result of this, on deformation the position of cross-links must be affinely transformed with respect to the macroscopical strain [3].

2) The phantom model provides maximal freedom to the network chains. The junctions are allowed to fluctuate freely about their mean positions [4]. If the junction fluctuations are changed by deformation the instantaneous cross-link positions are not longer affine with the macroscopical strain.

The affine and phantom models are now considered to provide the upper and lower limits of the mechanical response [5–7]. It is generally accepted that real networks should show a behavior intermediate between these two extremes.

From experiments it was deduced that at small strain, real networks show a behavior close to the affine model. At large deformation, on the other hand, phantom behavior should predominate. Accordingly, on moderate deformation a network should undergo a transition from affine to phantom behavior as is shown in Fig. 1.

In phenomenological terms this transition is often characterized with the aid of the Mooney-Rivlin equation [1, 2]. It is usually assumed that $2C_1$ is the modulus of the phantom network so that $2C_2$ may be taken as a measure of "non-phantomness" [7–9].

One of the purposes of the recent research on polymer networks is to understand the reasons behind the failure of known models. We believe that these attempts can be sucessful only if two fundamental aspects are accounted for:

i) Real network chains have volume and finite length;

ii) Topological constraints restrict conformational abilities of chains and junctions.

Until now, no molecular theory has dealt with both of these effects. Non-Gaussian approaches have been

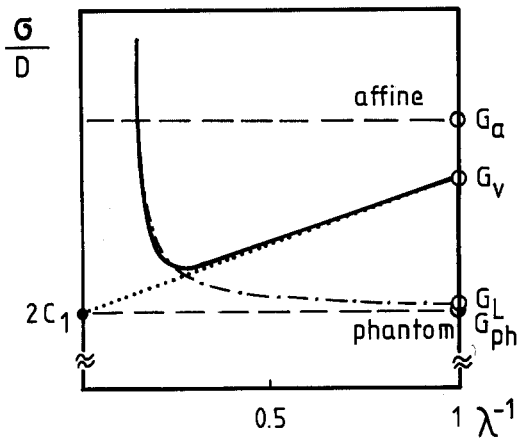

Fig. 1. A schematic diagram showing the dependence of reduced stress σ/D on reciprocal elongation. The phantom and affine network behaviors are represented by broken lines. The solid line stands for the real network behavior. The dotted line denotes the Mooney-Rivlin representation. (--) corresponds to the predictions of Langevin network model. The corresponding small strain moduli (G_{ph}, G_a, G_L, and G_v) are also presented

advanced taking finite chain extensibility into consideration [2,10,11]. With the aid of these theories it is in principle not possible to fit experimental data (see Fig. 1).

Using the entanglement concept, two different treatments are known: in the constrained junction fluctuation model entanglements are assumed to impose strain dependent restrictions onto fluctuations [7]. Tube and slip-link models lead to constraints affecting mainly conformational freedoms of chains [12,13,40,41].

Experimental evidence uniquely supporting the restricted fluctuation or slip-link concept has not been available until now. In these circumstances, it suggests itself to seek at least phenomenological modifications of the Gaussian network theory. Dossin and Graessley [14] introduced the phenomenological parameter h which is considered as an empirical measure for entanglement constraints onto fluctuation of junctions. The small strain modulus is rewritten as

$$G = (1 - 2h/f)\, G_a \tag{1}$$

where G and G_a stand for the modulus of real and affine networks, respectively, and f denotes the average functionality of cross-links. According to Eq. (1) the mean strain energy per chain is reduced by junction fluctuation. Complete suppression of junction fluctuation ($h = 0$) results in affine behavior – no suppression ($h = 1$) leads to the phantom network behavior. By defining Eq. (1) it is implicated that fluctuation of junctions play an increasingly minor role when the functionality of crosslinks is increased. The network should asymtoticaly approximate the affine deformation mode. The parameter h is often considered as an appropriate empiricall characterization of the non-Gaussian behavior of real networks [9,14,23]. Because of modifying the modulus only, the Dossin-Graessley characterization is reasonable at small strains only.

The van der Waals network equation of state [15] as a phenomenological modification of the Gaussian network theory accounts for finite chain extensibility and "global interactions". For simple extension the van der Waals equation of state reads

$$G = G_v\, D\, [D_m/(D_m - D) - aD] \tag{2}$$

where G_v is the van der Waals modulus, σ is the nominal stress. In Eq. (2) the deformation function, D, is defined by

$$D = \lambda - \lambda^{-2} \tag{3}$$

where λ is the strain ratio related to the unstrained system, measured in the direction of force. D_m is defined as D with λ replaced by the maximum strain λ_m which is related to the strain invariant unit of the network chains.

In Eq. (2) a denotes the phenomenological global interaction parameter. This parameter should include restrictions to junction fluctuation as well as topological entanglement constraints. It is important that the sigmoidal stress-strain curve of real networks can be fully fitted with the aid of van der Waals equation of state [15–17].

Eq. (2) has been cast into another form in order to be capable of describing every mode of deformation (simple extension, biaxial and triaxial deformational modes) [16]

$$G = G_v\, D\, [1/1(1 - \eta^{1/2}) - a_\phi \phi^{1/2}] \tag{4}$$

where $\phi = 1/2(I - 3)$ and I stands for the first strain invariant. $\eta = (I - 3)/(I_m - 3)$, where I_m denotes the maximum value of I. The relationship between the global interaction parameters is simply $a_\phi = \sqrt{2}\, a$.

The van der Waals parameters (a or a_ϕ and λ_m) can be deduced by appropriate calculation with the aid of Eqs. (2) or (4) applied to experiments. It turns out that

Table 1. The van der Waals and suppression of junction fluctuation parameters for some polymers. The h_v values were calculated by Eq. (17) with $f = 4$

system	a	λ_m	u	h_v
natural rubber	0.26	7.7	0.12	0.44
poly chloroprene	0.21	10.05	0.10	0.51
polybutadiene	0.24	12.5	0.16	0.08
TPR	0.24	11.0	0.15	0.18
SBR	0.19	13.5	0.11	0.46
PDMS	0.20	11.0	0.11	0.52
PVAc	0.26	6.8	0.11	0.49

the global interaction parameter does not vary considerably among networks with different crosslinking density. The van der Waals parameters for some polymers are listed in Table 1.

It seems to be of great interest to provide a comparison between the various models which take non-Gaussian effects into consideration. The main purpose of the present paper therefore is:

– to relate the phantom modulus and the van der Waals modulus;

– to interpret the finite chain-extensibility parameter of the van der Waals model with the aid of the Langevin model;

– to interpret the parameter which describes the suppression of junction fluctuation with the aid of the van der Waals model;

– to relate the parameters of the constrained junction fluctuation model with the van der Waals parameters.

In addition, effects of junction functionality on the mechanical properties will be discussed.

Experiments performed on dry networks will be described with the different models in order to come to a direct test of their abilities.

The relationship between the phantom modulus and van der Waals modulus

In order to relate the van der Waals modulus to the phantom modulus, we follow others [7, 9] in assuming that at large extension the reduced stress should reach the phantom network limit under the heuristical assumption of neglecting finite chain extensibility effects. In other words, the first Mooney-Rivlin coefficient ($2C_1$) is considered as the phantom network component of the real modulus. For small strains far below the finite chain extensibility region it is, of course, possible to express the Mooney-Rivlin coefficients in terms of the van der Waals parameters. For uniaxial extension Kilian and Vilgis derived the relations on the basis of Eq. (2) [17]

$$2C_1 = G_v\,(1-3u) \tag{5}$$

$$2C_2 = 3u\,G_v \tag{6}$$

where

$$u = (a - 1/D_m)\,. \tag{7}$$

It follows from $2C_1 = G_{ph}$ that the van der Waals modulus is then definied by

$$G_v = G_{ph}/(1 - 3u)\,. \tag{8}$$

The phantom modulus is related to the structural parameters of the network according to

$$G_{ph} = (1 - 2/f)\,\nu^* RT = G_o/\lambda_m^2 \tag{9}$$

where ν^* denotes the moles of network chains per unit volume. f stands for the junction functionality and G_o incorporates molecular characteristics of the polymer (bond angles, characteristic ratio, density) as well as the temperature.

The linear dependence of G_{ph} on ν^* is the consequence of equipartition of kinetical conformational energy. Equal amounts of free energy are stored by each of the chains in the Gaussian network. The stored free energy per network chain does not depend on the chain length or cross-linking density. This is not the case for van der Waals networks. Equation (8) says that the linear relationship between G_v and ν^* is lost.

A non-linear dependence of measured modulus on the cross-linking density is a well known phenomenon which is the subject of many discussions [1, 2, 9, 18, 23]. The effect is interpreted either by the non-completeness of cross-linking reaction, or by trapping of entanglements. In view of the meaning of the van der Waals parameters, it is concluded that the strain energy density (per chain) is modified by the global interactions and as a result, the small strain modulus is increased by a factor of $1/(1 - 3u)$ as predicted by Eq. (8).

Figure 2a shows the small-strain moduli as a function of concentration of network chains for randomly cross-linked poly(dimethylsiloxan) (PDMS) net-

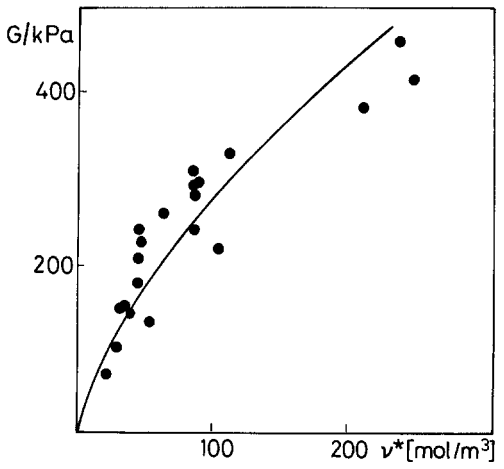

Fig. 2a. Small strain modulus G against concentration of network chains for tetrafunctional PDMS networks. The experimental data were taken from [23]. The solid line was calculated with the aid of Eq. (8) using the parameters $a = 0.2$, $G_o = 22$ MPa and $\nu^* = 13\,225/\lambda_m^2$

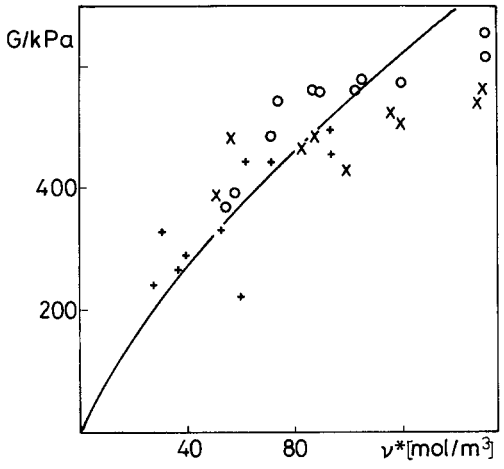

Fig. 2b. Small strain modulus versus concentration of network chains. + = natural rubber; ○ = polyisoprene (IR 98); × = polyisoprene (IR 92) random cross-linking by dicumyl peroxide. The experimental data of Gleim et al. were taken from [19]. The solid line was calculated with the aid of Eq. (8) using the parameters $a = 0.22$, $G_o = 36$ MPa and $\nu^* = 10^4/\lambda_m^2$

works with tetrafunctional crosslinks. The solid line was calculated with the aid of Eqs. (8) and (9) and the known van der Waals parameters listed in Table 1. For natural rubbers and polyisoprene networks the analogue representation is depicted in Fig. 2b. It is evidently seen that the non-linear relationship between G and ν^* can be described by our approach without introducing new parameters like, e.g., the trapping factor [18].

On the basis of our approach it is possible to formulate the Mooney-Rivlin equation in terms of van der Waals parameters

$$\frac{G}{D} = 2C_1 + 2C_1\, 3u/(1-3u)\, \lambda^{-1} \tag{10}$$

where the small strain modulus (G/D at $\lambda^{-1} = 1$) depends on the van der Waals parameters, while G_{Ph} or $2C_1$ (G/D at $\lambda^{-1} = 0$) is independent from u. This result is consistent with our assumption according to which only $2C_1$ (G_{Ph}) can be uniquely related to the cross-linking density. The small strain modulus (G_v) depends not only on the cross-linking density, but also on the global interaction parameter.

The Langevin and the van der Waals network models

The van der Waals equation of state implicates effects due to finite chain extensibility. It is interesting to ask under which circumstances Eq. (2) gives the Langevin type of behavior.

For a network of non-Gaussian (Langevin) chains the mechanical equation of state was derived [1, 2, 21, 22]. When λ_m is not too small the stress is written as

$$G = G_{Ph}\frac{\lambda_m}{3}\left[\beta_1 - \lambda^{-3/2}\beta_2\right] \tag{11}$$

where $\beta_1 = \mathscr{L}^*(\lambda/\lambda_m)$, $\beta_2 = \mathscr{L}^*(1/\lambda_m\lambda^{1/2})$ and $\bar{\mathscr{L}}^*(x)$ being the inverse Langevin function [11]. Introducing the series representation of $\mathscr{L}^*(x)$ [2]

$$\mathscr{L}^*(x) = 3x + 9/5\, x^3 + 297/175\, x^5 + 1539/875\, x^7 + \ldots + \tag{12}$$

we are led at small strains to the Langevin modulus

$$G_L = G_{ph}\,(1 + 6/5\, \lambda_m^2). \tag{13}$$

Taking it for granted that the maximum strain parameter, λ_m, is identical in both approaches and combining Eqs. (8) and (13), we are led to the ratio of the Langevin modulus to that of the van der Waals model

$$\frac{G_L}{G_v} = \frac{5\lambda_m^2 + 6}{5\lambda_m^2}\,(1-3u). \tag{14}$$

Both moduli coincide if $a = a_L$

$$a_L = 2/(5\lambda_m^2 + 6) + 1/D_m \cong 1/D_m \qquad (15)$$

where a_L is used as adjusting parameter. Since the first term in Eq. (15) is usually much smaller than the second one, it is possible to approximate a_L with $1/D_m$. In Fig. 3 model calculations for three networks with different cross-linking density are shown in the Mooney-Rivlin fashion. It can be seen that the van der Waals equation of state with a proper choice of a is able to cover the Langevin type behavior fairly well. For moderate simple extension the "Langevin $2C_2$" is in principle negative, in contradiction with the experimental findings from which $2C_2 > 0$ was always deduced. Figure 4 shows the stress-strain dependence for natural rubber cross-linked in undiluted state [33], as well as for poly(vinyl acetate) network prepared at high dilution (v_c = 0.08 wt%), but measured in dry state. Although solution cross-linked networks are supposed to have smaller degrees of entangling, in PVAc networks $2C_2$ is observed to not be diminished. Not only in simple extension, but also at unidirectional compression, large values of $2C_2$ have been reported (see Figs. 4 and 10). Non-zero $2C_2$s may be taken as manifestation of "global interactions" which seem to occur in any case, independent of how the networks have been prepared, in dry or in swollen state.

These results underscore that just regarding finite chain extensibility does not lead to a perfect theoretical fit to the experimental data. Other effects, possibly due to junction fluctuation and entanglements, must be accounted for.

In terms of the van der Waals model it is possible to separate the finite chain extensibility and the global interaction effects by rewriting Eq. (2)

$$G = G_v\,[D + D^3/[D_m(D_m - D)] - uD^2]\,. \qquad (16)$$

The first term in brackets represents the ideal (Gaussian) behavior, the second stands for the Langevin correction, and the third one for the global interactions.

The quantity u can be considered as the "cross-linking density-dependent effective global interaction parameter". Since $2C_2$ is proportional with u (see Eq. (6)), positive $2C_2$ requires $u > 0$, that is, $a > 1/D_m$. Within the scope of our knowledge this inequality is supported by experimental results (Table 1).

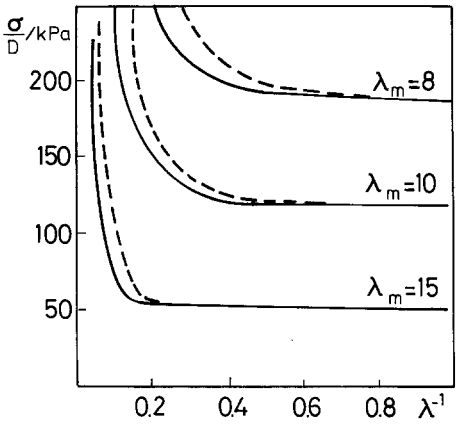

Fig. 3. Mooney-plot for Langevin (—) and for van der Waals (- -) networks. The inverse Langevin function as approximated by Treloar [2]

$$\mathscr{L}^*(x) = 3x/(1 - 0.6x^2 - 0.2x^4 - 0.2x^6)$$

is used. The van der Waals data were computed with the aid of Eq. (2) using the parameters $a = a_L$ (Eq. (15)) and $G_{ph} = 12\,000/\lambda_m^2$. The three different degrees of crosslinking are characterized by λ_m. The value of this parameter is indicated with each curve

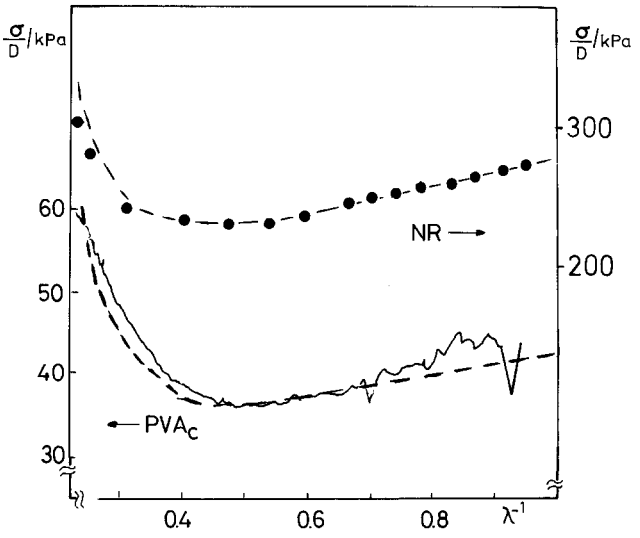

Fig. 4. Mooney-Rivlin plot for vulcanized rubber (●), (the data were taken from [33]), and for PVAc network (—) prepared in solution, measured in dry state. (- -) denotes reduced stress calculated with the aid of van der Waals equation of state, Eq. (2). The parameters are given in Table 1

The relationship between the supression of junction fluctuation parameter and the van der Waals corrections

Since both the Dossin-Graessley- and the van der Waals-approach describe the true moduli, it suggests itself to relate their phenomenological parameters. By combining Eqs. (1) and (8) with $G_v = G(h)$ and $G_{ph} = (1-2/f)G_a$ we arrive at $(h = h_v)$

$$h_v = (2-3uf)/(2-6u). \tag{17}$$

In Table 1 the van der Waals corrections and the calculated h_v are presented for some networks. On the basis of these data h_v is between 0 and 1 in accordance with the expectation. Deduced in a completely different manner, Dossin and Graessley found for polybutadiene rubbers $h = 0$ [14], which compares fairly well with $h_v = 0.08$. For tetrafunctional PDMS networks, Queslel and Mark reported Graessley parameters in the range of $0.13 < h < 0.588$ [9], while Gottlieb et al. arrived at $h = 0.69$ [23]. This again is in good correspondence with $h_v = 0.52$.

According to our approach the parameter of suppression of junction fluctuation seems not to have the general meaning it was supposed to have [14]. According to Dossin and Graessley, h should not vary appreciably among different networks. On the basis of Eq. (17) we expect, on the contrary, rather strong effects if the cross-linking density or the junction functionality is varied. This finding is in agreement with the recent results of Queslel and Mark (9). The PDMS networks show a decisive dependence of h on the cross-linking density and average junction functionality. Table 2 shows strong influence of the molecular mass of network chains on the Dossin-Graessley parameter of end-linked PDMS networks. Values calculated on the basis of Eqs. (7) and (17) are shown for comparison. Despite uncertainties in a and D_m, the van der Waals approach gives the basic trend.

Table 2. Dependence of the parameter of suppression of junction fluctuation on the molecular mass (M_n) of the network chains of trifunctional end-linked PDMS networks. h_v was calculated by Eq. (17) with $f = 3$, $a = 0.24$ and $\lambda_m = 0.1 \cdot M_n^{1/2}$

M_n	h	h_v
4000	0.99	0.82
4700	1	0.79
9500	0.61	0.64
11300	–	0.52
18500	0.15	0.49
25600	0.13	0.43
32900	0.21	0.37

The dependence of the global interaction parameter on the junction functionality

It is well known that the junction functionality plays an important role in rubber elasticity. It was found that $2C_2$ decreases with increasing junction functionality [26]. In case of filler networks, multifunctionally cross-linked model networks constituted by only tying the filler particles to the polymer matrix with many bonds, negative $2C_2$ s were deduced from simple extension experiments [24].

With the aid of van der Waals' equation of state it is possible to discuss crosslink functionality effects. This was already done by Kilian et al. [34] by introducing an empirical relation between the global interaction parameter and the junction functionality.

To describe quantitatively the $a(f)$ dependence we use the result of Vilgis and Kilian [25]. They have, on the basis of modelling the interaction on permanent crosslinks as a scattering problem, shown that $2C_2$ can be written as

$$2C_2 = 3G_a\left[\alpha_c \frac{(f-1)^2}{f^3} - 1/D_m\right] \tag{18}$$

where α_c is a characteristic constant. Its value can be determined from the global interaction parameter at known junction functionality (see Eq. (19)). By combining Eq. (18) with Eqs. (1), (6), (7), and (8) we arrive at

$$a(f) = \frac{\alpha_c \dfrac{(f-1)^2}{f^3} - \dfrac{1}{D_m}}{\dfrac{f-2}{f} + 3\alpha_c\left[\dfrac{(f-1)^2}{f^3} - \dfrac{1}{D_m}\right]} + 1/D_m. \tag{19}$$

It follows from Eq. (19) that as the functionality increases, the global interaction parameter decreases. In the limit $f = \infty$ we are led to $a = -3/[D_m(D_m - 3)]$, which is practically zero for not too short chain networks.

With the aid of Eq. (19) it is predicted that affine behavior predominates if the junction functionality is large. According to Eq. (1) the quantity $2h/f$ controls the ratio of G/G_a. Since the global interaction parameter depends on the functionality, the suppression of

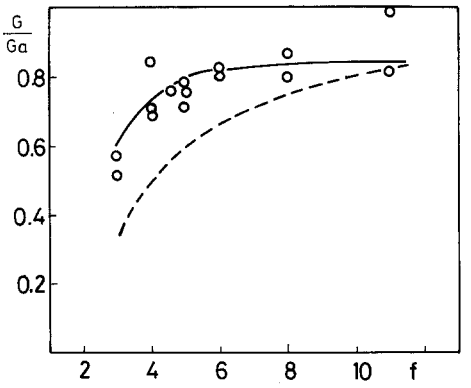

Fig. 5. G/G_a against the junction functionality f for end-linked PDMS networks. O denotes the experimental points of Llorente and Mark [26]. The solid line is calculated by Eq. (1), taking into account the functionality effect by Eqs. (17) and (19). For the calculation, $\lambda_m = 11$ and $a(f = 4) = 0.2$ are used. The dotted line represents the phantom network behavior

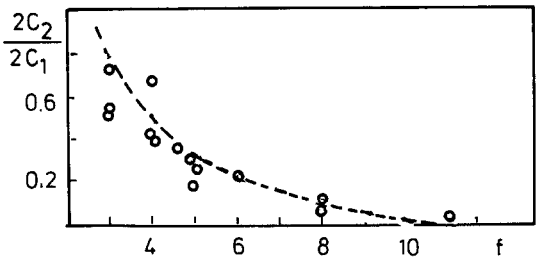

Fig. 6. $2C_2/2C_1$ as a function of junction functionality f for end-linked PDMS networks [26]. The dotted line is calculated by Eqs. (19) and (20) with the parameters $a(f = 4) = 0.2$ and $\lambda_m = 11$

junction fluctuation parameter should also dependend on f. Queslel and Mark have reported that for trifunctional endlinked PDMS networks h was found to be much larger than for tetrafunctional ones [9]. The $a(f)$ dependence modifies the ratio G/G_a accordingly. This effect is shown in Fig. 5. It is to be seen by evidence that the deviation of experimental data from the phantom network behavior is rather significant at small strains. By calculations with the aid of the van der Waals model, the experimental data can fairly well be fitted.

Not only the modulus, but also the whole stress-strain pattern is influenced by the junction functionality which is fully reproduced with the aid of our approach.

It is customary to consider the ratio of $2C_2/2C_1$ as a measure of deviation from the Gaussian theory. With the help of Eqs. (5) and (6) it is possible to relate $2C_2/2C_1$ to the van der Waals parameters

$$2C_2/2C_1 = 3u(f)/[1 - 3u(f)]. \tag{20}$$

According to Eqs. (19) and (20), $2C_2/2C_1$ is predicted to decrease with increasing functionality. That this holds true is demonstrated in Fig. 6 on the basis of experimental data from Mark and Llorente [26]. It can be seen that calculations with the van der Waals model deliver a rather good description. According to Eq. (20) there is a critical functionality predicted at which $2C_2/2C_1$ dissapears. $2C_2/2C_1$ switches beyond this limit to a negative sign. This mechanical "theta-point situation" is bound to the condition $u(f) = 0$, which is fulfilled if

$$(f-1)^2/f^3 = 1/(\alpha_c D_m). \tag{21}$$

In the case of regular networks α_c lays between 1 and 2, establishing $D_m = 10$; the change in the sign of $2C_2$ should occur between $10 < f < 20$. In this matter, the behavior of "filler networks" is of interest. These model networks are constituted only by introducing chemical silica-to-rubber bonds to filler particle [24]. Functionality and mass of the "junctions" have very large values (200–400 bonds per filler particle of a mean radius of about 5–10 nm). For these networks very negative $2C_2$ s have been deduced [24].

Comparison of van der Waals- and constrained junction fluctuation models at unidirectional extension

The constrained junction fluctuation model developed by Flory and Erman [7] is based on the assumption that in real networks the diffusion of junctions may be severely restricted by neighboring chains sharing the same region of space. At small strains entanglement constraints onto junctions should predominate and the stress is larger than for a phantom network. Constraints should then be released at higher deformation, so that restrictions onto junction fluctuation should vanish. The phantom network behavior is approximated in this limit. In the Flory-Erman model the parameter $\varkappa$ measures the severity of entanglement constraints and ξ characterizes the non-affine transformation of the domains of constraints with strain. The phantom limit corresponds to $\varkappa = 0$, while affine deformation should occur at $\varkappa = \infty$.

For dry networks ξ is usually very small, becoming less important than $\varkappa$; ξ is therefore often set to zero.

The stress-strain relation is given by

$$G = G_{ph}\, D\, [1 + [\lambda K(\alpha_1^2) - \lambda^{-2} K(\alpha_2^2)]\, D^{-1}] \quad (22a)$$

where

$$K(\alpha_t) = \frac{B_t}{(1+B_t)} \frac{\partial B_t}{\partial \alpha_t} + \frac{B_t g_t}{(1+B_t g_t)} \frac{\partial (B_t g_t)}{\partial \alpha_t^2} \quad (22b)$$

$$g_t = \alpha_t^2\, [\varkappa + \xi(\alpha_t - 1)] \quad (22c)$$

$$B_t = (\alpha_t - 1)\, [1 + \alpha_t - \xi \alpha_t^2]\, (1 + g_t)^{-2}$$

$$t = 1, 2\,. \quad (22d)$$

The principal components of strain $\alpha_t = \alpha_1$ and $\alpha_t = \alpha_2 = \alpha_3$ are

$$\alpha_1 = \lambda \left(\frac{V}{V_o}\right)^{1/3} \quad (22e)$$

$$\alpha_2 = \alpha_3\, \lambda^{-1/2} \left(\frac{V}{V_o}\right)^{1/3}. \quad (22f)$$

In Eqs. (22e, f) V_o refers to the volume at which the crossliks are introduced.

Despite the molecular interpretation given for $\varkappa$ and ξ, these parameters do not follow from the theory itself; their values must be deduced by fitting stress-strain experiments.

From Eq. (22a) the small strain modulus is derived to be defined [9] by

$$G = G_{ph} \cdot [1 + H(\varkappa, \xi)] \quad (23a)$$

where

$$H(\varkappa, \xi) = \frac{1}{4} \left(2 - \xi\right)^2 \frac{\varkappa^2 (\varkappa^2 + 1)}{(\varkappa + 1)^2}. \quad (23b)$$

By comparing Eqs. (23a, b) with Eq. (8) one arrives at

$$u = \frac{1}{3} \frac{H(\varkappa, \xi)}{1 + H(\varkappa, \xi)}. \quad (24)$$

This result strongly supports the assumption of Kilian [15] that the global interaction parameter should be governed by restrictions to the junction fluctuations.

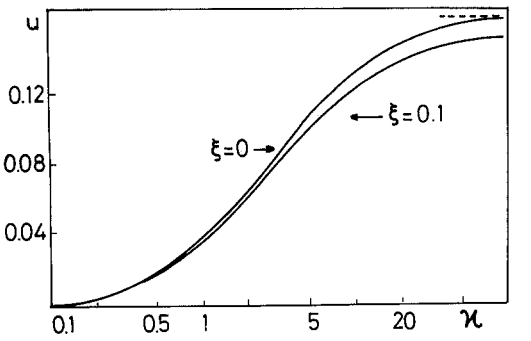

Fig. 7. The dependence of effective global interaction parameter on the parameters of constrained junction fluctuation model. The dotted line denotes the upper limit of u

Figure 7 shows how the effective global interaction parameter depends on the measure of severity of entanglement constraints, calculated with the aid of Eq. (24) at two different values of ξ. It becames clear that the entanglement effect by which the junction is restricted ($\varkappa \to \infty$) should enlarge the global interaction parameter until its upper limit is reached. This results in that both sides of Eq. (24) are functions of the crosslinking density, the lefthand side via D_m and the righthand side via $\varkappa$. When the crosslinking density is increased, $\varkappa$ decreases. According to Eq. (24) u must then become smaller as well.

For networks with a small junction functionality ($f = 4$), the constrained junction fluctuation model delivers an upper and a lower limit of u

$$0 < u = (a - 1/D_m) < 1/6\,. \quad (25)$$

According to Table 1 this inequality seems to be satisfied by experiment.

On the basis of Eq. (24) stress-strain behavior of the van der Waals approach can now be compared with the constrained junction fluctuation model. Figure 8 presents the Mooney-plot for crosslinked natural rubbers according to Mullins [33]. In the Flory-Erman representation with $\xi = 0$, $\varkappa$ was computed with the aid of Eqs. (23b) and (24) by using the known van der Waals parameters. At small strains, $\lambda^{-1} = 1 - 0.5$, the data computed with the aid of the van der Waals- and the constrained junction fluctuation theory are in satisfactory agreement. At large strains, $\lambda^{-1} < 0.5$, only the van der Waals equation of state fits the typical upturn.

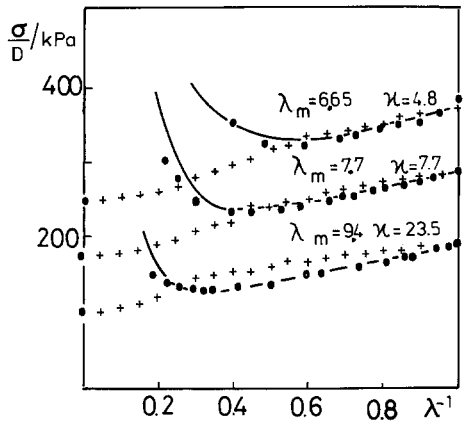

Fig. 8. Mooney-plot of measurements on natural rubber according to Mullins [33]. + = calculated by Eq. (22a); − = calculated by Eq. (2) ($a_\phi = 0.34$). The additional parameters used in the calculations are indicated with each curve

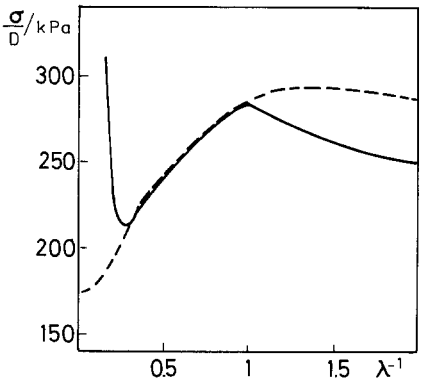

Fig. 9. Reduced stress versus strain according to the constrained junction fluctuation (– –), and to the van der Waals (—) model. The parameters are: $G_{ph} = 175$ kPa, $\varkappa = 8$. The global interaction parameter $a_\phi = .32$ is deduced from Eq. (24) with $\xi = 0$ and $\lambda_m = 10$

The stress-strain dependence of dry networks at unidirectional compression

The mechanical behavior of dry rubber-like materials at unidirectional compression has continued to be the subject of controversial discussions. For different molecular theories rather different stress-strain patterns are computed.

The constrained junction fluctuation model [7], as well as the tube model of Gaylord [27] predict in the Mooney-Rivlin representation a maximum lying in the compression region. The slip-link model [13] gives no maximum and positive $2C_2s$. The primitive path approach [28] yields negative $2C_2s$.

The experimental findings are also controversial. Results obtained on natural rubber [29], on PDMS networks [30, 35], and on polyurethane elastomer [43] deliver, in general, negative $2C_2s$. Mark et al. found, on the other hand, that PDMS networks prepared in solution and studied afterwards in the unswollen state show positive $2C_2s$. Oppermann and Rennar deduced for end-linked PDMS networks positive $2C_2s$ as well [32].

In Fig. 9 calculations are depicted which are carried out with the aid of the constrained junction fluctuation model, and with the van der Waals equation of state. In order to relate the parameters of these models to each other, Eq. (24) was used. At small and moderate extensions the agreement is excellent. At large extensions, where finite chain extensibility comes into play, one can of course observe large differences. These two approaches deliver a completely different behavior under uniaxial compression. It is now crucial that the constrained junction fluctuation model predicts a maximum, and the van der Waals model, a minimum at intermediate strains (which is not to be seen in Fig. 9). At small compression $2C_2$ is positive for the Flory-Erman theory, while the van der Waals model yields to negative $2C_2s$.

It is a crucial test to make accurate compression measurements at very small uniaxial strains ($1 < \lambda^{-1} < 1.5$–2). Figs. 10a, b show small strain compressional data of PVAc networks prepared in solution, measured in dry state. These PVAc networks have apparently negative $2C_2s$ under compression. These results support the van der Waals concept. The problem remains for the correct interpretation of the careful measurements of Oppermann and Rennar [32].

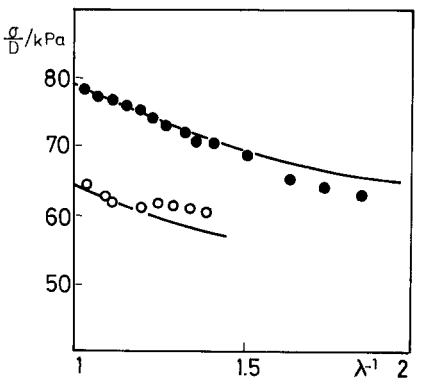

Fig. 10a. Mooney-Rivlin plot for PVAc networks which were prepared in the highly diluted state, but measured in the dry state. The solid lines were calculated by Eq. (4) with the parameters $a_\phi = 0.34$, $\lambda_m = 15$ (●), and $\lambda_m = 20$ (○), respectively

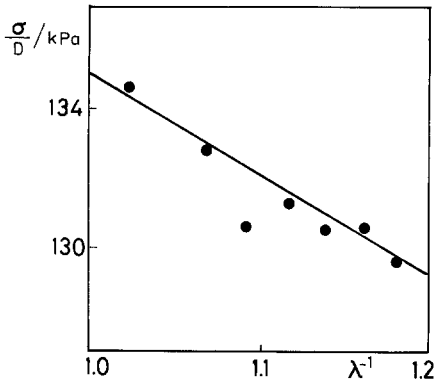

Fig. 10b. Mooney-plot in the unidirected compression region of a PVAc network prepared in highly diluted state, measured in dry state. The dotted line was calculated by Eq. (4) with the parameters $a_\phi = 0.34$ and $\lambda_m = 9.8$

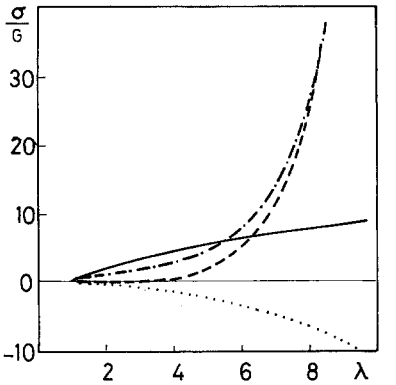

Fig. 11. Non-Guassian stress-strain components in comparison with the Gaussian behavior (—). Finite chain (Langevin) correction (– – –) and interaction correction (. . .) was calculated with the aid of the second and third terms in Eq. (16), respectively. The stress-strain dependence for a real (van der Waals) network (– · –) was calculated by Eq. (16) with $a = 0.2$ and $\lambda_m = 10$

Conclusions

Let us briefly summerize some of the significant results:

— The new formulation of the van der Waals modulus delivers a non-linear dependence of the small strain modulus on the crosslinking density in accord with observation.

— The global interaction parameter can be related to the junction functionality.

— The suppression of junction fluctuation parameter, h, can be interpreted in terms of the van der Waals parameters. It comes out that h_v should depend on the cross-linking density and the junction functionality.

— By comparing the van der Waals and the constraint junction fluctuation models, the entanglements constraint-parameters can be expressed in terms of the van der Waals parameters.

— In the region of small- and moderate extensions the van der Waals and the Flory-Erman theories give the same result. At large deformations only the van der Waals equation of state delivers a quantitative representation of experimental data.

— In the region of unidirectional compression the van der Waals model is characterized by negative $2C_2s$ being in accord with experiments on dry PVAc networks.

In view of these results the relevance of two non-Gaussian effects, finite chain extensibility and global interaction among network chains, is beyond doubt. These two effects play a different role at different strains. This illustrated with the plot in Fig. 11. At small strains the finite chain correction (the second term in Eq. (16)) is negligibly small so that mainly the global interaction term (the third part in Eq. (16)) makes its influence felt. Finite chain extensibility induces the sharp upturn in the vicinity of $\lambda = \lambda_m$. It is interesting to note that finite chain effects give, in principle, a positive correction of the Gaussian behavior, while the global interaction (the fluctuation) term, on the other hand, reduces the "ideal" stress. Both non-Gaussian effects together lead to a minimum behavior at moderate deformations. This can be seen in Fig. 12. At small strains the negative interaction term overpowers the

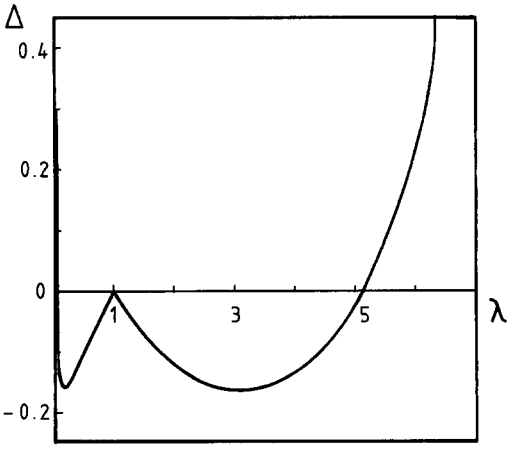

Fig. 12. Deviation Δ from the ideal stress-strain behavior as a function of strain. $\Delta = (G_{vdW} - G_{ph})/G_{ph}$ was calculated with the aid of Eq. (4) using the parameters $a = 0.2$ and $\lambda_m = 10$

finite chain effects. As the strain increases this negative term is gradually compensated, becoming finally smaller than the finite chain correction. At a certain deformation, where the relationship holds

$$\phi^{1/2} = u_\phi \phi_m^{1/2}/(1 + u_\phi \phi_m) \tag{26}$$

where

$$u_\phi = a - 1/\phi_m^{1/2} \tag{27}$$

both terms compensate each other: the network seems to behave like an affine network.

In conclusion, it must be emphasized that finite chain effects and interactions between chains and junctions are both important. It is imperative for every molecular theory of rubber elasticity to take this into consideration. The recent papers of Edwards and Vilgis [40, 41] who developed a combined version of the tube and slip-link models, might be seen as a step in this direction.

Experimental

Unidirectional extension and compression measurements were performed on poly(vinyl acetate) (PVAc) networks. The PVAc samples were obtained by acetylation of poly vinyl alcohol (PVA) gels. These gels according to a previously described method [36–38] were prepared by crosslinking of aqueous PVA solutions having concentrations, v_c, between 6–12 wt %, with glutaric dialdehyde. The acetylation was performed in a mixture of 40 vol % acetic anhydride, 50 vol % pyridine and 10 vol % acetic acid at a temperature of 90 °C for 8 h. After acetylation the swollen networks were washed in acetone. The acetone was renewed several time until the reactants of acetylation were completely removed. Cylindrical samples to be used in unidirecitonal compression, and films for simple extension measurements were prepared. The swollen gels were carefully dried at 60 °C.

Dry cylindrical samples (diameter 0.4–0.8 cm, height 0.4–0.8 cm) were unidirectionally compressed by using a homemade apparatus [39]. This equipment enables determination of force and deformation in the range of 0.1 mN to 2 N, and 6 μm to 3.33 mm, with an accuracy of 0.1 mN and 6 μm, respectively. The reproducibility of mechanical measurements, including sample preparation, was better than 8 %.

Since the PVAc has a glass temperature at $Tg = 32$ °C, the compressional measurements were performed at 60 °C. At each stress we waited 5 h until mechanical equilibrium was attained. The simple extension was performed at 100 °C by using the Zwick 1445 equipment.

Acknowledgment

One of us (M.Z.) wishes to thank the Alexander von Humboldt Foundation for financial support while these studies were carried out. This work was partly supported by grants from the Hungarian Academy of Science (AKA and OTKA No = 1-3-86-229, No = 1204/86).

References

1. Flory PJ (1959) Principles of Polymer Chemistry. Cornell University Press, Ithaca
2. Treloar LRG (1967) The Physics of Rubber Elasticity. Clarendon Press, Oxford
3. Kuhn W (1936) J Chem Phys 76:258
4. James H, Guth E (1947) J Chem Phys 15:669
5. Graessley W (1975) Macromolecules 8:186
6. Doi M, Edwards SF (1978) J Chem Soc Faraday Trans 2, 74:1802
7. Erman B, Flory PJ (1982) Macromolecules 15:800
8. Ronca G, Allegra G (1975) J Chem Phys 63:4990
9. Queslel JP, Mark JE (1984) Adv Polym Sci 65:137
10. Smith TL (1977) Treatise on Materials Science and Technology. Ed Schultz JM 369
11. Kovac J, Crabb C (1982) Macromolecules 15:537
12. Ball RC, Doi M, Edwards SF, Warner M (1981) Polymer 22:1010
13. Marrucci G (1979) Rheol Acta 18:123
14. Dossin LM, Graessley W (1979) Macromolecules 12:123
15. Kilian HG (1981) Polymer 22:209
16. Kilian HG, Unseld K, Jaeger E, Müller J, Jungnickel B (1985) Colloid Polym Sci 263:607
17. Kilian HG, Vilgis T (1984) Colloid Polym Sci 262:15
18. Langley NR (1968) Macromolecules 1:348
19. Gleim W, Oppermann W, Rehage G (1986) Makromol Chem 187:1273
20. Mark JE, Sullivan JL (1977) J Chem Phys 3:1006
21. James HM, Guth E (1943) J Chem Phys 11:455
22. Guth E (1966) J Polym Sci C 12:89
23. Gottlieb M, Macosco CW, Benjamin GS, Meyers KO, Merril EW (1981) Macromolecules 14:1039
24. Kilian HG, Schenk H, Wolff S (1987) Colloid Polym Sci 265:410
25. Vilgis T, Kilian HG (1986) Colloid Polym Sci 264:137
26. Lorente MA, Mark JE (1980) Macromolecules 13:325
27. Gaylord RJ (1982) Polym Bull 8:325
28. Edwards SF (1977) Br Polym J 9:140
29. Rivlin RS, Saunders DW (1951) Phil Trans R Soc London A 243:251
30. Pak H, Flory PJ (1979) J Polym Sci 17:184
31. Chen RYS, Yu CU, Mark JE (1973) Macromolecules 6:746
32. Oppermann W, Rennar N (1987) Progr Colloid Polym Sci 75:49
33. Mullins L (1959) J Appl Polym Sci 2:257
34. Kilian HG, Enderle HF, Unseld K (1986) Colloid Polym Sci 264:866
35. Gottlieb M, Macosko CW, Lepsch TC (1981) J Polym Sci 19:1603
36. Horkay F, Nagy M, Zrinyi M (1980) Acta Chim Acad Sci Hung 103:387
37. Zrinyi M, Horkay F (1982) J Polym Sci Phys 20:815
38. Horkay F, Zrinyi M (1984) Macromolecules 17:2805
39. Horkay F, Nagy M, Zrinyi M (1981) Acta Chim Acad Hung 108:287
40. Edwards SF, Vilgis TH (1986) Polymer 27:483

41. Edwards SF, Vilgis TH (1988) Rep Prog Phys 51:243
42. Kilian H-G (1980) Polym Bull 3:151
43. Chompff AJ (1977) Chemistry and Properties of Crosslinked Polymers. Academic Press, New York, San Francisco, London p 375

Received September 30, 1988;
accepted November 4, 1988

Authors' addresses:

Prof. Dr. H.-G. Kilian
Universität Ulm
Abt. Experimentelle Physik
Oberer Eselsberg
D-7900 Ulm, F.R.G.

Dr. M. Zrinyi
L. Eötvös University
Department of Colloid Science
Puskin u. 11-13
H-1088 Budapest, Hungary